Harmful Thermal Radiation and Bending Effects on Power Attenuations in Deformed Plastic Optical Fibers

Ahmed Nabih Zaki Rashed[1], A. Abd El-Naser Mohamed[2], Imbaby I. Mahmoud[3], , Mohamed S. El_Tokhy[4], Osama H. Elgzar[5]

[1,2]Electronics and Electrical Communication Engineering Department, Faculty of Electronic Engineering, Menouf, 32951, Egypt

[3,4,5]Engineering Department, Nuclear Research Center, Atomic Energy Authority, P.O. 13759, Inshas, Egypt

Abstract—*Radiation and temperature influence the optical fiber characteristics. These influences such as increasing the power loss were studied and shown to result from the refractive index changes occurring within the fibers induced by bending and thermal effects. In this paper we present a model and a simulation results to reveal the effect of radiation and temperature on the bent polymer optical fiber by using Vissim environment. We demonstrate the importance of operating wavelength and optical fiber parameters in the reduction of the power losses. This formulated treatment provides a mean to control the optical characteristics of fibers in radiation environments. The results are validated against published experimental work and showed good agreement.*

Keywords─ Gamma radiation, thermal irradiation effect, critical bend radius parameters, polymer optical fiber, power loss.

I. INTRODUCTION

The growth of internet traffic in the past decade has led to an increasing demand for data transmission capacity media even in local area networks (LANs) and home networks [1]. Optical fiber is the basic element in the modern high capacity and high-bit-rate optical telecommunication systems [2-3] There are many types of optical fibers such as glass fibers and plastic fibers [4].Plastic optical fibers (POFs) are being considered for high-performance fiber links at very short distances than silica based fibers because of their ductility, light weight [5], low cost, flexibility and ease of handling and interconnecting [1]. Furthermore they have much higher bandwidth [6] they are resistance to impacts and vibrations [7]. In addition due to the large fiber cross-section of plastic optical fires, connecting to the light source and detector is non-problematic [8-9]. Additionally they are providing reliable data transmission in such diverse fields as industrial and residential local-area networks, home and office applications [10]. However particularly in such local area networks (LANs), many fiber bendings and junctions are inevitable [11]. This result in radiation losses occur at bends in the fiber path. At a bend, the geometry of the core-cladding interface changes and some of the guided light is transmitted from the core into the cladding [12-13]. Zubia and Arrue studied the effects of bending on the power attenuation of POFs and found that the radiation losses observed in bent fibers are a result primarily of refraction of the meridional rays [14]. The average plastic-energy density (APED) accumulated in a deformed POF could result in radiation loss and scattering loss. However it provides a key index for evaluating the power loss in the deformed fiber [14]. Furthermore due to plastic optical fiber advantages it is being considered for use in many systems. Many of these applications require operation in nuclear radiation environments. That is commonly known as it introduces a highly damaging to optical waveguides [15]. Furthermore radiation induced effects in materials and devices are evaluated based on the energy losses resulting upon the interaction between highly energetic radiation and matter [16-18]. Thus when the polymer is subjected to ionizing radiation, it undergoes several changes in its physical and chemical structures induced by radiation, leading to cross linking and scission of molecules phenomena that occur simultaneously, and one of them prevails over the other depending on various factors, such as, material type, irradiation dose and irradiation atmosphere [19-23]. Such polymers are known as degrading polymer [1]. In addition to these effects ionizing radiation will be absorbed, reflected and transmitted in varying degrees, according to the physical properties of the materials on which it falls. The portion which is absorbed will cause a rise in temperature [24]. which plays a significant role in the number of reactions that take place during/after irradiation

as a rise in 10°C can double the reaction rates [25].In general, ionizing radiation, ambient temperature and loading deformation change the geometry of the original POF [14]. Therefore, it is necessary that the power loss characteristics of bent polymer optical fibers under high-temperature and radiation conditions are well understood [10]. Consequently, we are interested with evaluation of power loss that enables us to calculate the poverty that occurs in optical fiber transmission characteristics such as in the MH-4001 and GH-4001 fibers which are intended for digital home appliance interfaces and automotive and machinery control applications, respectively under high thermal irradiation environment. In addition, it allows predicting operating wavelength, thermal and radiation harmful effect. The arising effects of bending, temperature and ionizing radiation on power loss are obligatory in designing high-bit-rate optical communication systems such as in local area networks (LANs) and home networks.

This work was done by using VisSim environment. VisSim is a Windows-based program for modeling and simulating complex dynamic systems. VisSim combines an intuitive drag-and-drop block diagram interface with a powerful simulation engine. The visual interface offers a simple method for constructing, modifying, and maintaining complex system models. Furthermore, all modeling and simulation tasks can be completed without writing a line of code. This leads to significant savings in both development time and costs, and a greater assurance that the resultant product will perform as specified.

This paper is organized as follows: Section II presents the basic assumptions and modeling of radiation induced dispersion, Section III describes the model results. However section IV is devoted to conclusion.

II. BASIC ASSUMPTIONS AND MODELING OF THERMAL RADIATION CRUEL EFFECT ON POWER LOSS OF BENT POLYMER OPTICAL FIBER

In this work a block diagram model treating the radiation and temperature effects on power loss of bent polymer optical fibers is proposed to estimate the power losses in the MH-4001 and GH-4001 optical fibers which are two SI POFs, under a given set of deformation, temperature, and radiation doses taking into consideration critical bend radius parameters. The core and cladding of the POFs are fabricated from polymethyl methacrylate (PMMA) and fluorinated polymer, respectively. The light source is a light-emitting diode launched directly into the front end of the fiber and it is assumed to overfill the fiber so that all mode groups are present. The power delivered to a POF before deformation is denoted as P_{in}. The output power of deformed fiber is denoted as P_{out}. Therefore for the MH-4001 and GH-4001 POFs, it can be shown that the power ratio P_{out}/P_{in} is related to the APED $\bar{u}_p$, via the following expression [14].

$$\frac{P_{out}}{P_{in}} = 10^{\{-c(T)\exp[-d(T)R]\}}\left(-a(T)\bar{u}_p^2 - b(T)\bar{u}_p + 1\right) \quad (1)$$

where R and $\bar{u}_p$ are bend radius (millimeters "mm") and average plastic energy density (Newton millimeter per cubic millimeters "N mm – mm^{-3}") respectively, and the coefficients a (T), b (T), c (T) and d (T) are temperature functions with the forms:

for the MH-4001 fiber

$$a(T) = 3.53\times10^{-6}T + 5.94\times10^{-4} \quad (2)$$

$$b(T) = 5.56\times10^{-4}T - 6.78\times10^{-3} \quad (3)$$

$$c(T) = -1.56\times10^{-2}T + 1.898 \quad (4)$$

$$d(T) = -3.06\times10^{-4}T + 0.235 \quad (5)$$

However for the GH-4001 fiber

$$a(T) = 3.53\times10^{-6}T + 5.44\times10^{-4} \quad (6)$$

$$b(T) = 4.71\times10^{-4}T - 5.34\times10^{-3} \quad (7)$$

$$c(T) = -1.92\times10^{-2}T + 2.066 \quad (8)$$

$$d(T) = -5.63\times10^{-4}T + 0.248 \quad (9)$$

Moreover the radius of curvature of fiber bend is critical to the amount of power lost [12]. So the minimum bending radius must be defined [26], because the losses are negligible until the radius reaches a critical size that is the minimum bending radius [12].

$$R_C = \frac{3n_2\lambda}{4\pi(NA)^3} \quad (10)$$

Where λ, NA, and n_2 stand for the operating wavelength, numerical aperture and the clad refractive index of the optical fiber respectively. Therefore, equation (1) can be simplified as follows

$$\frac{P_{out}}{P_{in}} = 10^{\{-c(T)\exp[-d(T)R_C]\}}\left(-a(T)\bar{u}_p^2 - b(T)\bar{u}_p + 1\right) \quad (11)$$

Moreover to demonstrate the effect of gamma radiation on the power loss characteristics of bent polymer optical fiber we will use Sellmeier formula. Since the refractive index of any optical material can be interpolated by the Sellmeier formula, which has a physical basis based in the Lorentz oscillator model [27]. So the refractive index of material base fiber link can be expressed as a function of temperature T,

$$n^2(T,\lambda,\gamma) = A(T,\gamma) + \frac{B(T,\gamma)\lambda^2}{\left(\lambda^2 - C(T,\gamma)\right)} + \frac{D(T,\gamma)\lambda^2}{\left(\lambda^2 - E\right)}$$

operating optical signal wavelength λ and irradiation fluencies of Gamma rays γ as the following formulas [28].

(12)

where λ, T, and γ denote the wavelength, temperature, and irradiation fluencies of Gamma rays respectively. The first and second terms represent the contributions to the refractive index due to the higher and lower energy gaps of electronic absorption band, respectively, and the last term accounts for the lattice vibrational absorption. The constant E is not critical since the material stop transmitting long before the onset of the lattice absorption frequency. Usually, it is used the value $100\mu m^2$ [29]. Therefore, equation (11) can be simplified as follows [28].

$$n(T,\lambda,\gamma)=\left[A(T,\gamma)+\frac{B(T,\gamma)\lambda^2}{\left(\lambda^2-C(T,\gamma)\right)}+\frac{D(T,\gamma)\lambda^2}{\left(\lambda^2-E\right)}\right]^{1/2} \quad (13)$$

where the coefficients A(T,γ), B(T,γ), C(T,γ) and D(T,γ) are temperature and radiation dose functions with the forms

$$A(T,\gamma)=A(\gamma)F_A(T) \quad (14)$$

$$B(T,\gamma)=B(\gamma)F_B(T) \quad (15)$$

$$C(T,\gamma)=C(\gamma)F_C(T) \quad (16)$$

$$D(T,\gamma)=D(\gamma)F_D(T) \quad (17)$$

However the coefficients A (γ), B (γ), C (γ) and D (γ) are radiation dose functions with the forms

$$A(\gamma)=1.329631+2.7\times10^{-4}\exp\left(\frac{\gamma}{0.319319}\right) \quad (18)$$

$$B(\gamma)=0.82863+7.7\times10^{-4}\exp\left(\frac{\gamma}{0.440013}\right) \quad (19)$$

$$C(\gamma)=0.01105+4.7\times10^{-6}\exp\left(\frac{\gamma}{0.391139}\right)\mu m^2 \quad (20)$$

$$D(\gamma)=0.98481+1.1\times10^{-3}\exp\left(\frac{\gamma}{0.964926}\right) \quad (21)$$

Where γ is the radiation dose in MGy. Although the coefficients $F_A(T)$, F_B (T), F_C (T) and F_D (T) are temperature functions with the forms

$$F_A(T)=\frac{1.338922-3.7\times10^{-4}(T-T_0)}{1.338922} \quad (22)$$

$$F_B(T)=\frac{0.819526-3.843\times10^{-4}(T-T_0)}{0.819526} \quad (23)$$

$$F_C(T)=\frac{0.011127-3.1\times10^{-6}(T-T_0)}{0.011127} \quad (24)$$

$$F_D(T)=\frac{1.055995-2.8\times10^{-3}(T-T_0)}{1.055995} \quad (25)$$

where T ,T_0 donate ambient temperature, and the room temperature respectively, finally the second order differential equation of the optical fiber core refractive index is given by

$$\frac{d^2n}{d\lambda^2}=-0.25\frac{\left[\frac{2B\lambda}{\lambda^2-C}-\frac{2B\lambda^3}{\left(\lambda^2-C\right)^2}+\frac{2D\lambda}{\lambda^2-E}-\frac{2D\lambda^3}{\left(\lambda^2-E\right)^2}\right]^2}{n^{\frac{3}{2}}}$$

$$+0.5\frac{\left[\frac{2B}{\lambda^2-C}-\frac{10B\lambda^2}{\left(\lambda^2-C\right)^2}+\frac{8B\lambda^4}{\left(\lambda^2-C\right)^3}+\frac{2D}{\lambda^2-E}-\frac{10D\lambda^2}{\left(\lambda^2-E\right)^2}+\frac{8D\lambda^2}{\left(\lambda^2-E\right)^3}\right]}{n} \quad (26)$$

Hence the cladding refractive index can be obtained via the following relation [29].

$$n_2=0.9979n \quad (27)$$

where n, n_2 donate core, and clad refractive index respectively.

III. RESULTS AND DISCUSSION

We have demonstrated the power attenuation characteristics of bent polymer optical fiber deformed under gamma radiation dose ranging from 0.1 to 3MGy and temperature ranging from 25 to 80 ^{0}C taking into consideration critical bends radius parameters. We clarify the harmful effect of thermal irradiation environments and critical bend radius parameters on power loss characteristics. The results show that that a larger APED accumulated in the de-formed POF can result in a larger radiation loss and scattering loss, and a higher temperature results in a lower power losses. The reference values of these parameters are shown in Table 1. These values of the calculations are taken from [10], [12], [14] and [28].

Table 1: Operating parameter's values used in the model were as the following

Operating parameter	Symbol	Value
Radiation dose	γ	0.1-3.0 MGy
Ambient temperature	T	25 - 80 ^{0}C
Operating wavelength	λ	850-1550 nm
Room temperature	T_0	25 ^{0}C

Clad refractive index	n_2	1.2-1.5
Numerical aperture	NA	0.2-0.5

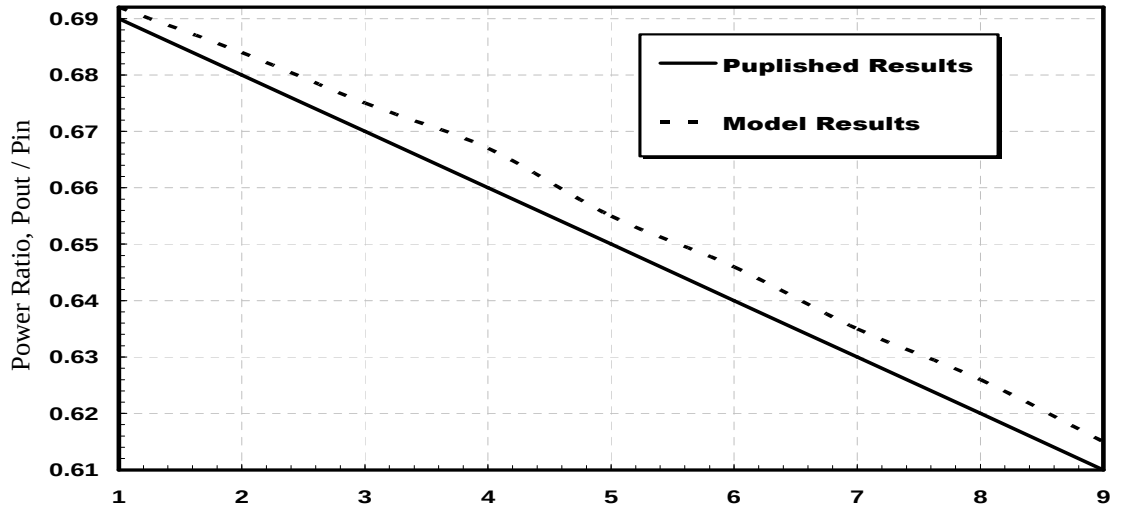

Fig.1. Variations of the power ratio against average plastic energy density with T=25 ^{0}C and R= 10 mm.

In figure (1) reveals the typical computed values for the power ratio against average plastic energy density under the thermal irradiation environment effect, and experimental values are represented in the above figure that shows a good agreement between the resulted curve and the published experimental curve.

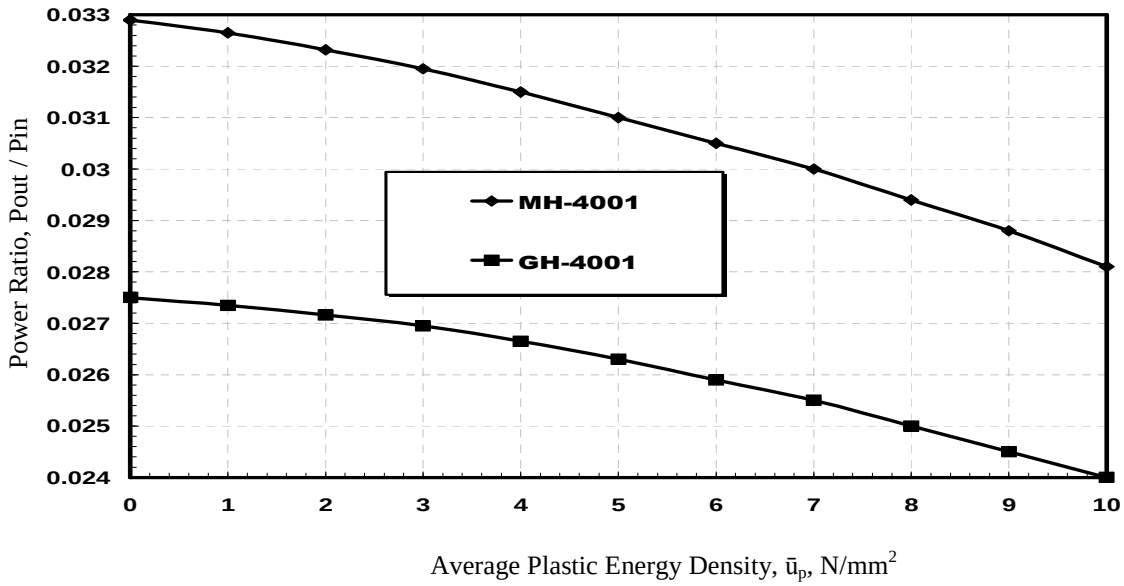

Fig.2. Variations of the power ratio against average plastic energy density with T=25 ^{0}C, γ =0.1MGy, and λ=1310 nm.

Figure (2) shows that the power ratio decreases (power loss increases) with the increasing of the average plastic energy density, this is because of a larger APED accumulated in the deformed POF implies that a larger stress is accumulated in the fiber this can result in a non-uniform distribution of the refractive index along the fiber core, which in turn introduces refraction and reflection phenomena which causes radiation and scattering losses. Thus the power ratio decreases with increase the APED. Furthermore the figure shows also that the power loss increment in MH-4001 is much than GH-4001this is because The coating diameters measured at necking position for GH-4001 and MH-4001 fibers are 1.98 and 1.96 respectively, (L. W. Chen etal., 2009) [14]. This

means the diameter shrinkage in the GH-4001 fiber is smaller than that in the MH-4001. This is why the power loss increment in the deformed MH-4001 fiber is greater than that in the GH-4001 fiber. But still the MH-4001 fiber is a higher power ratio than GH-4001 fiber, at constant temperature (T =25 ^{o}C).

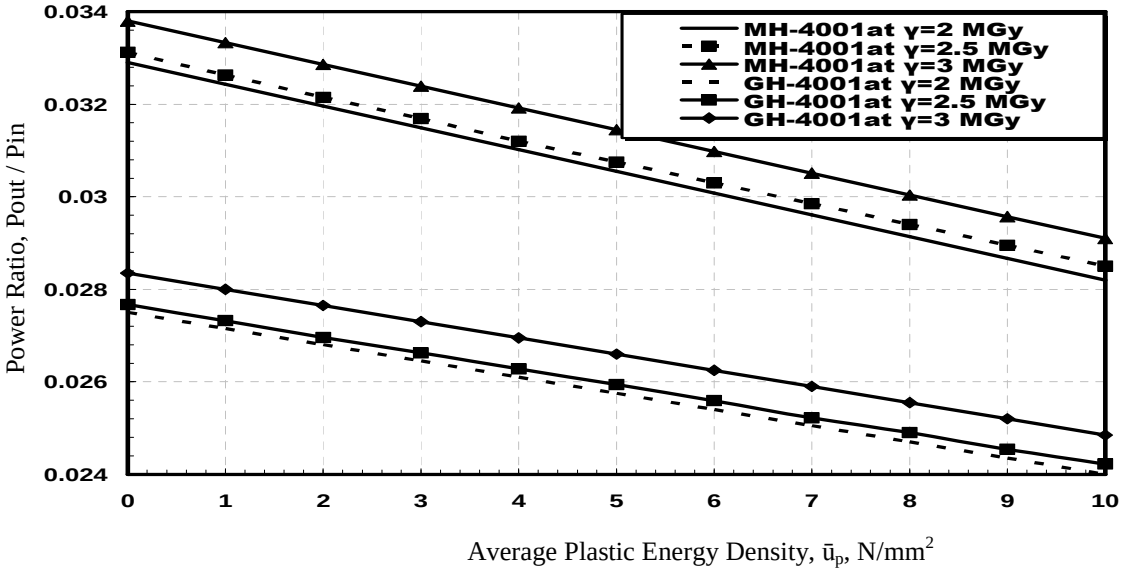

Fig.3. Variations of the power ratio against average plastic energy density at different radiation doses (γ) with T=25 0C, NA = 0.2, and λ=1310 nm.

Figure (3) shows that the two fibers suffer lower power losses at higher radiation doses. This result can be accredited to the reduction in the accumulated plastic energy in the deformed fibers as the deformation radiation dose is increased, since the plastic energy stored in the fiber, decreases with increasing radiation dose. Moreover a lower value of the APED reduces the scattering losses in the deformed POF since a smaller stress accumulated in the fiber can result in a smaller variation of the refractive index along the fiber core [14]. Furthermore, a lower APED value implies that the POF experiences a smaller geometrical deformation and thus suffers smaller radiation losses. Hence, the two fibers exhibit lower power losses at higher radiation dose. Figures from 4-6 depicts the relationship between the power losses in the POFs and the APED value as a function of the critical bend radius parameters.

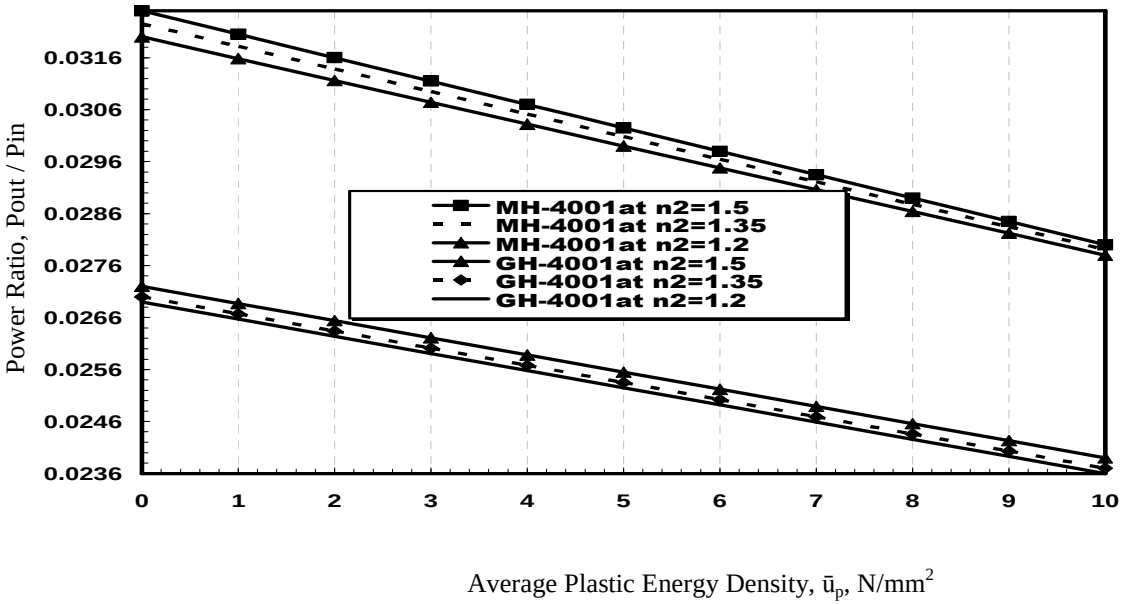

Fig.4. Variations of the power ratio against average plastic energy density at different clad refractive index (n_2) with T=25 ^{0}C, γ = 0.1 MGy, and λ=1310 nm.

Figure (4) reveals that the power ratio decreases as the value of the refractive index of the optical fiber clad (n_2) decrease at constant APED. This result can be accredited to smaller clad refractive index will results in large acceptance angle which is a figure that represents a fiber light gathering capability. However the change in the rays' paths as they travel in bent fibers due the geometry change of the original POF as a result of both the ambient temperature and the loading deformation, and consequently induces radiation losses. Furthermore, the stresses within a POF subjected to bending and elongation forces are not distributed uniformly, but vary along the length of the core. The resulting inhomogeneous distribution of the refractive index leads to scattering losses [14]. The higher acceptance angle indicates that more modes we have this means that greater radiation and scattering losses this is due to the change in the rays' paths as a result of the loading deformation and inhomogeneous distribution of the refractive index and therefore there are more of them. So that lower clad refractive index fiber results in high power loss.

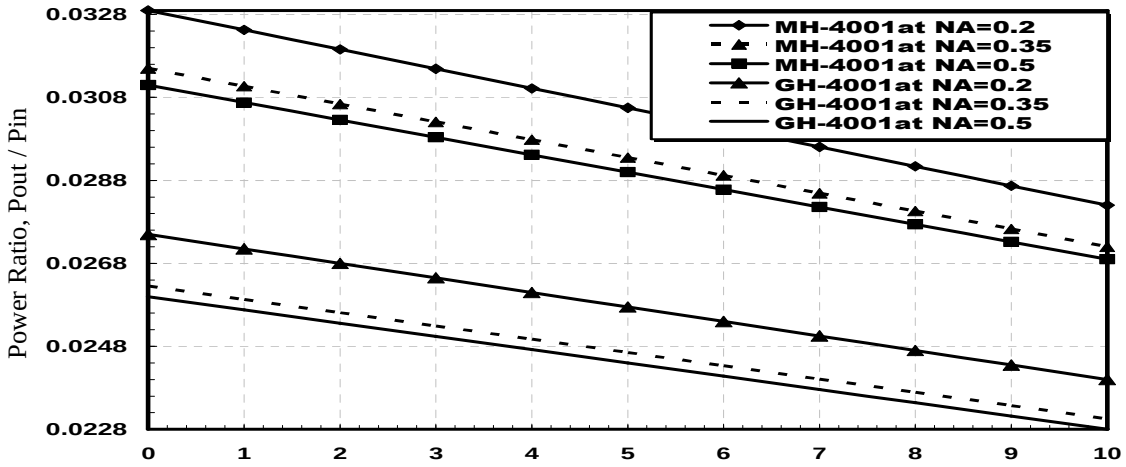

Fig.5. Variations of the power ratio against average plastic energy density at different numerical aperture (NA) with T=25 ^{0}C, γ = 0.1 MGy, and λ=1310 nm.

Figure (5) reveals that the power ratio decreases as the value of the numerical aperture (NA) of the optical fiber increase at constant APED. This result can be attributed to the change in the rays' paths as they travel in bent fibers due the geometry change of the original POF as a result of both the ambient temperature and the loading deformation, and consequently induce radiation losses. Furthermore, the stresses within a POF subjected to bending and elongation forces are not distributed uniformly, but vary along the length of the core. The resulting inhomogeneous distribution of the refractive index leads to scattering losses [14]. The higher NA indicates that more modes we have this means that greater radiation and scattering losses this is due to the change in the rays' paths as a result of the loading deformation and inhomogeneous distribution of the refractive index and therefore there are more of them. So the power loss increases in larger NA fibers.

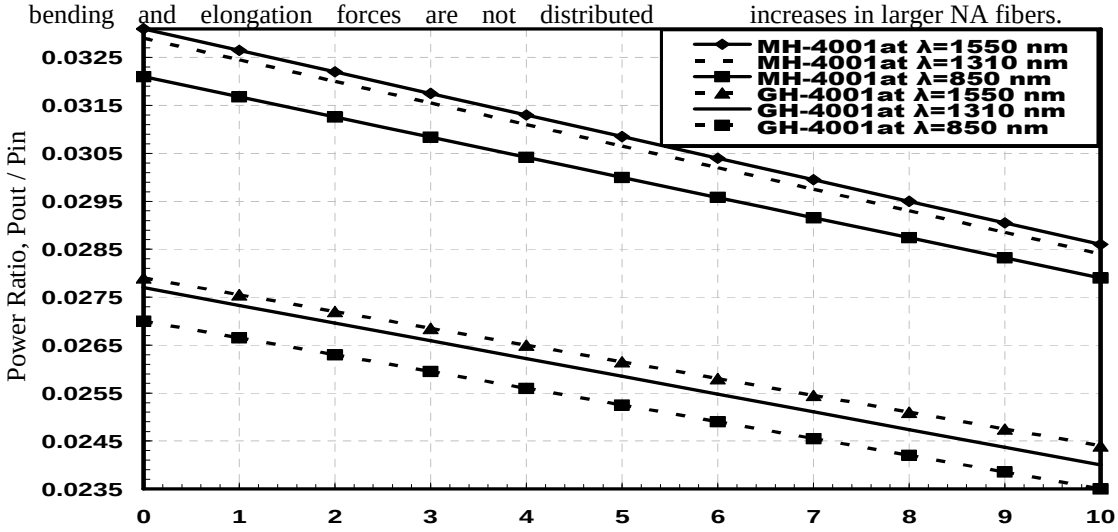

Average Plastic Energy Density, $\bar{u}_p$, N/mm^2

Fig.6. Variations of the power ratio against average plastic energy density at different operating wavelengths (λ) with T=25 ^{0}C, γ = 0.1 MGy, and NA=0.2.

Figure (6) shows that the power ratio decreases as the value of the operating wavelength (λ) decrease at constant APED. This result can be attributed to the change in the rays' paths as they travel in bent fibers due the geometry change of the original POF as a result of both the ambient temperature and the loading deformation, and consequently induce radiation losses. Furthermore, the stresses within a POF subjected to bending and elongation forces are not distributed uniformly, but vary along the length of the core. The resulting inhomogeneous distribution of the refractive index leads to scattering losses [14]. the operation at short wavelength means at the same time the operation at high frequency thus the higher frequency, the wider the bandwidth which indicates that more modes we have which give the ability of sending more complex information this means that greater radiation and scattering losses this is due to the change in the rays' paths as a result of the loading deformation and inhomogeneous distribution of the refractive index and therefore there are more of them. So the power losses increases with increase the bandwidth or decrease the operating wavelength since wider bandwidth indicates that there are more rays that carry information in the fiber**.** However with increasing the average plastic energy density which implies that the POF experiences a larger geometrical deformation and thus suffers higher radiation losses.

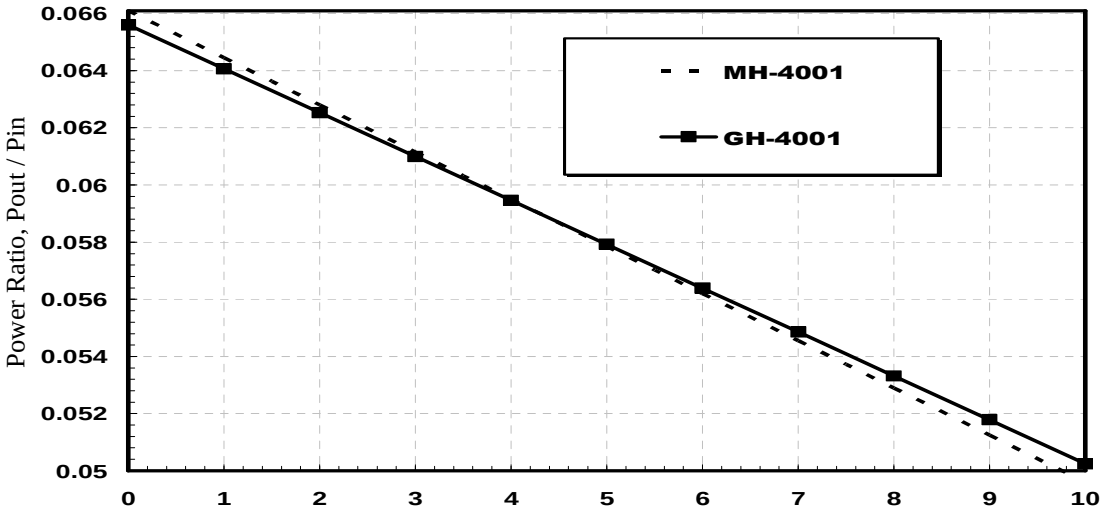

Fig.7. Variations of the power ratio against average plastic energy density at T=45 ^{0}C, γ=0.1MGy, and λ=1310 nm.

Figure (7) shows that the when the temperature increase from 25 ^{o}C to 45 ^{o}C MH-4001 fiber is still has a higher power ratio than GH-4001 fiber but with increasing the average plastic energy density which implies that the POF experiences a larger geometrical deformation and thus suffers higher radiation losses the GH-4001 fiber exhibits a greater resistance to power losses under high deformation conditions than MH-4001 fiber. This means that, the power loss in the deformed GH-4001 fiber is less than that in the MH-4001 fiber. This is due to the diameter shrinkage in the GH-4001 fiber is smaller than that in the MH-4001. This is why the power ratio in the deformed GH-4001 fiber is greater than that in the MH-4001 fiber. Furthermore figure (7) shows that the two fibers have higher power ratio at higher temperatures. This is because the reduction in the accumulated plastic energy in the deformed fibers as the deformation temperature is increased (from 25 to 45 ^{0}C). A lower value of the APED reduces the scattering losses in the deformed POF since a smaller stress accumulated in the fiber can result in a smaller variation of the refractive index along the fiber core. Furthermore, a lower APED value implies that the POF experiences a smaller geometrical deformation and thus suffers smaller radiation losses. Hence, the two fibers exhibit lower power losses at higher temperatures, as shown in Fig. 7.

Figure (8) shows that the power ratio decreases with the increasing of the average plastic energy density for two fibers, this is because of a larger APED accumulated in the deformed POF implies that a larger stress is

accumulated in the fiber this can result in a non-uniform distribution of the refractive index along the fiber core, which in turn introduces refraction and

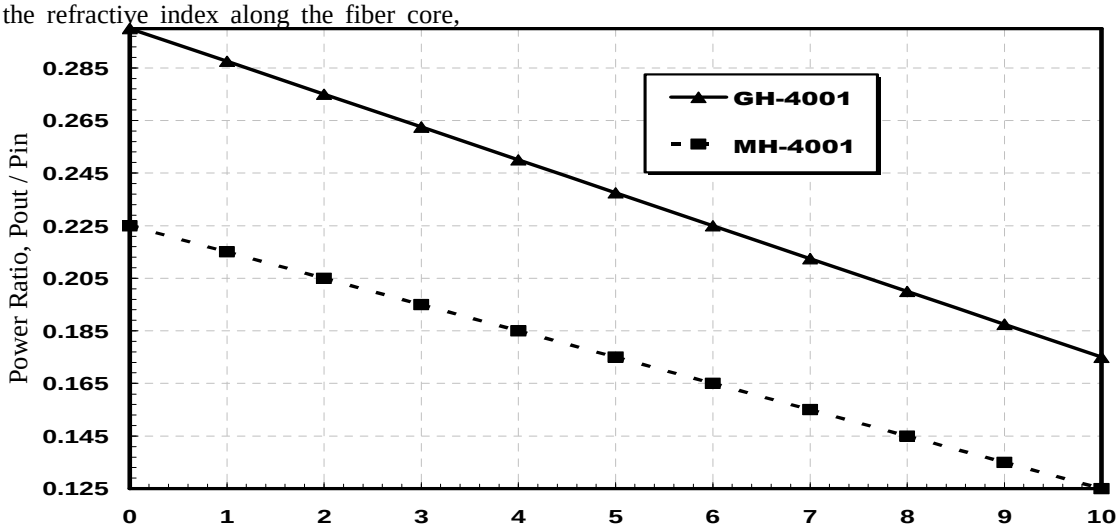

reflection phenomena which causes the incident rays to scatter in all directions. Thus the power losses increase with increase the APED. Furthermore the figure shows also that GH-4001 fiber has higher power ratio than MH-4001 fiber. Moreover the GH-4001 fiber maintains this improved power loss resistance under high deformation temperatures (T =80 oC). This is because the GH-4001 fiber has a higher glass transition temperature (Tg) than the MH-4001 fiber. A thermo-mechanical analysis machine (TMA, PerkinElmer, USA) is used to measure the Tg of the two fibers, and the values of 64.1 and 60.8 0C are recorded for the GH-4001, and MH-4001 SI POF cores, respectively , (L. W. Chen etal., 2009) [14]. This shows that the GH-4001 has the highest Tg value and implies that the chain motion in the GH- 4001 is less significant than in the other materials. It means that the polymer chain of the GH-4001 is more rigid than this of the MH-4001. Moreover it can be concluded that the GH-4001 fiber has smaller diameter shrinkage and a higher Tg than the MH-4001 fiber. This is why the power loss in the deformed GH-4001 fiber is less than that in the MH-4001 fiber. Furthermore figure (12) shows that the two fibers have higher power ratio at higher temperatures than in figure (2) and figure (7). This is because the reduction in the accumulated plastic energy in the deformed fibers as the deformation temperature is increased (T = 80^0C). A lower value of the APED reduces the scattering losses in the deformed POF since a smaller stress accumulated in the fiber can result in a smaller variation of the refractive index along the fiber core. Furthermore, a lower APED value implies that the POF experiences a smaller geometrical deformation and thus suffers smaller radiation losses. Hence, the two fibers exhibit lower power losses at higher temperatures, as shown in Fig. 12.

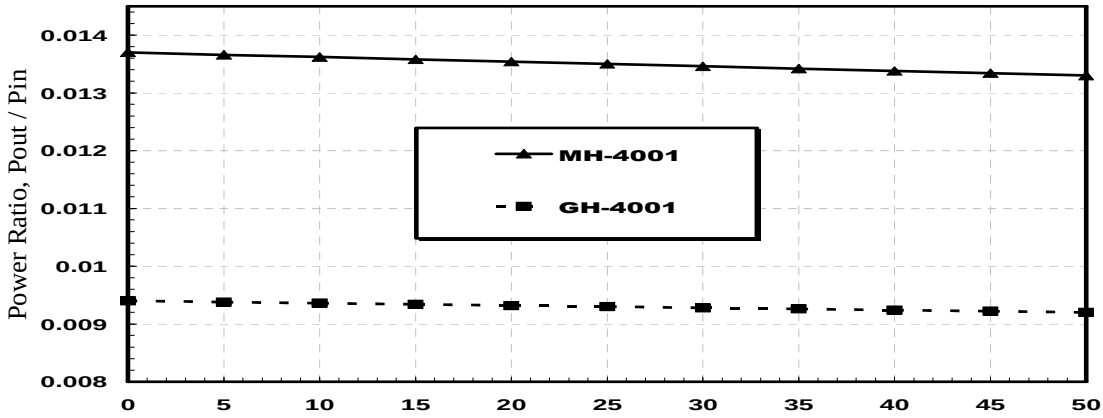

Fig.9. Variations of the power ratio against temperature with ($\bar{u}_p$ =1 N/mm^2), γ=0.1MGy, and λ=1310 nm.

Figure (9) shows that the power ratio decreases with the increasing of the ambient temperature at constant value of average plastic energy density ($\bar{u}_p$ =1 N/mm^2) and radiation dose (γ =0.1 MGy). It is as a result of the change in the rays' paths as they travel in bent fibers due the geometry change of the original POF as a result of both the ambient temperature and the loading deformation, and consequently induces radiation losses. Furthermore, the stresses within a POF subjected to bending and elongation forces are not distributed uniformly, but vary along the length of the core. The resulting inhomogeneous distribution of the refractive index leads to scattering losses [14]. Thus the power losses increases with increase the ambient temperature, Moreover the figure shows also that MH-4001 fiber is a higher power ratio than GH-4001 fiber, at constant low average plastic energy density ($\bar{u}_p$ =1 N/mm^2). Furthermore the power loses in MH-4001 increase rapidly than that in GH-4001. In the same time GH-4001 fiber maintains this improved power loss resistance under high deformation temperature. This is because the GH-4001 fiber has a higher glass transition temperature (Tg) than the MH-4001 fiber. Furthermore it implies that the chain motion in the GH- 4001 is less significant than in the other materials. It means that the polymer chain of the GH-4001 is more inflexible than this of the MH-4001. Moreover with increasing the average plastic energy density which implies that the POF experiences a larger geometrical deformation and thus suffers higher radiation losses the GH-4001 fiber exhibits a greater resistance to power losses under high deformation conditions than MH-4001 fiber. This is due to the diameter shrinkage in the GH-4001 fiber is smaller than that in the MH-4001 fiber which make the power ratio in the deformed GH-4001 fiber is greater than that in the MH-4001 fiber. The smaller diameter shrinkage and higher glass transition temperature (Tg) interprets why the power loss increment in the deformed GH-4001 fiber is less than that in the MH-4001 fiber.

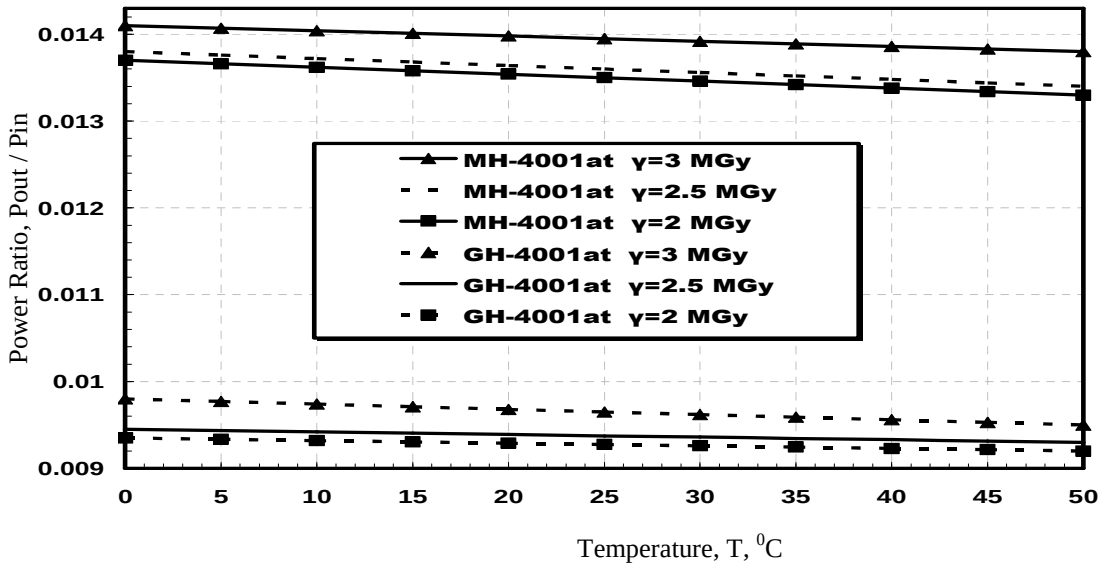

Fig.10. Variations of the power ratio against temperature at different radiation doses (γ) with ($\bar{u}_p$ =1 N/mm^2), NA=0.2, and λ=1310 nm.

Figure (10) shows that the two fibers suffer lower power losses at higher radiation doses at constant value of average plastic energy density ($\bar{u}_p$ =1 N/mm^2). This result can be accredited to the reduction in the accumulated plastic energy in the deformed fibers as the deformation radiation dose is increased, since the plastic energy stored in the fiber, decreases with increasing radiation dose. Moreover a lower value of the APED reduces the scattering losses in the deformed POF since a smaller stress accumulated in the fiber can result in a smaller variation of the refractive index along the fiber core [14]. Furthermore, a lower APED value implies that the POF experiences a smaller geometrical deformation and thus suffers smaller radiation losses. Hence, the two fibers exhibit lower power losses at higher radiation dose. Moreover the figure shows that the power ratio decreases with increase the ambient temperature at constant average plastic energy density ($\bar{u}_p$ =1 N/mm^2). Furthermore the power loses in MH-4001 increase rapidly than that in GH-4001. In the same time GH-4001 fiber maintains this improved power loss resistance under high deformation radiation dose. This is because the GH-4001 fiber has a

higher glass transition temperature (Tg) than the MH-4001 fiber. Furthermore it implies that the chain motion in the GH- 4001 is less significant than in the other materials. It means that the polymer chain of the GH-4001 is more inflexible than this of the MH-4001. This is why the power loss increment in the deformed GH-4001 fiber is less than that in the MH-4001 fiber. However, the two fibers are still exhibit power losses at higher radiation dose.

Figures 11-13 show the relationship between the power losses in the POFs and the ambient temperature as a function of the critical bend radius parameters.

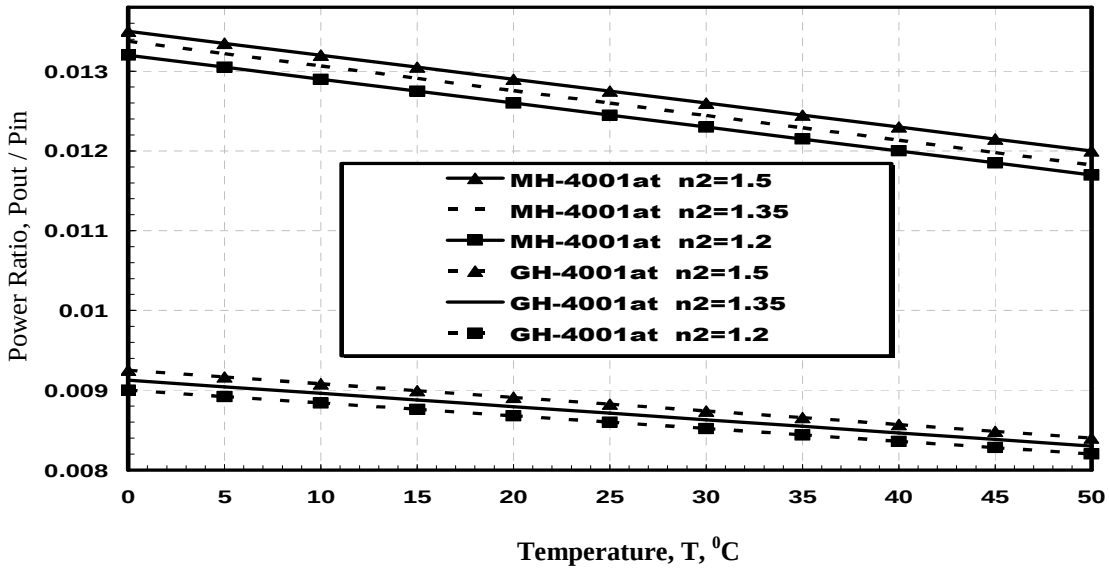

Fig.11. Variations of the power ratio against temperature at different clad refractive index (n_2) with ($\bar{u}_p$ =1 N/mm^2), NA=0.2, and λ=1310 nm.

Figure (11) reveals that the power ratio decreases as the value of the refractive index of the optical fiber clad (n_2) decrease at constant value of average plastic energy density ($\bar{u}_p$ =1 N/mm^2) and radiation dose (γ =0.1 MGy). This result can be accredited to smaller clad refractive index will results in large acceptance angle which is a figure that represents a fiber light gathering capability. However the change in the rays' paths as they travel in bent fibers due the geometry change of the original POF as a result of both the ambient temperature and the loading deformation, and consequently induces radiation losses. Furthermore, the stresses within a POF subjected to bending and elongation forces are not distributed uniformly, but vary along the length of the core. The resulting inhomogeneous distribution of the refractive index leads to scattering losses [14]. The higher acceptance angle indicates that more modes we have this means that greater radiation and scattering losses this is due to the change in the rays' paths as a result of the loading deformation and inhomogeneous distribution of the refractive index and therefore there are more of them. So that the power loses increase in a lower clad refractive index fiber. Furthermore the power loses in MH-4001 increase rapidly than that in GH-4001. In the same time GH-4001 fiber maintains this improved power loss resistance under high deformation temperature. This is because the GH-4001 fiber has a higher glass transition temperature (Tg) than the MH-4001 fiber. Furthermore it implies that the chain motion in the GH- 4001 is less significant than in the other materials. It means that the polymer chain of the GH-4001 is more inflexible than this of the MH-4001. This is why the power loss increment in the deformed GH-4001 fiber is less than that in the MH-4001 fiber.

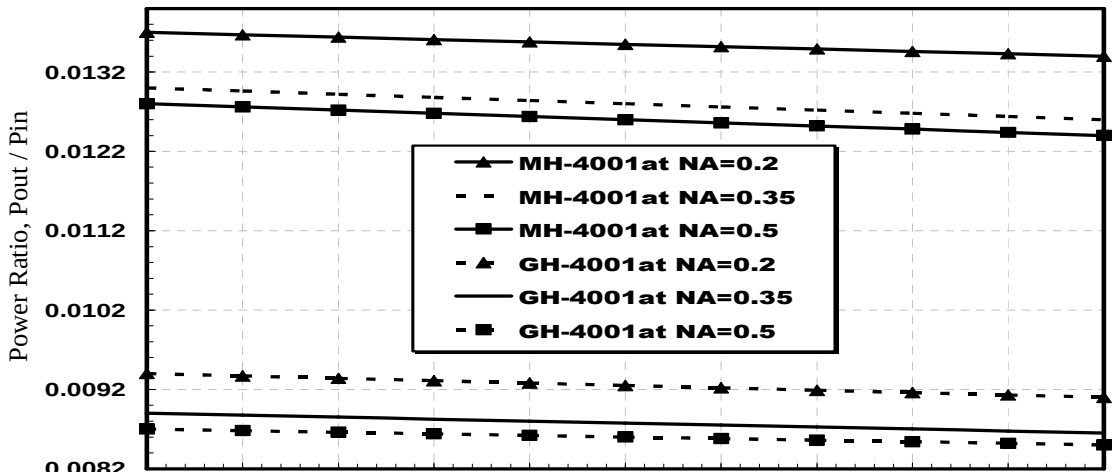

Temperature, T, ^{0}C

Fig.12. Variations of the power ratio against temperature at different numerical aperture (NA) with ($\bar{u}_p$ =1 N/mm^2), γ = 0.1 MGy, and λ=1310 nm

Figure (12) reveals that the power ratio decreases as the value of the numerical aperture (NA) of the optical fiber increase at constant value of average plastic energy density ($\bar{u}_p$ =1 N/mm^2) and radiation dose (γ =0.1 MGy). This result can be attributed to the change in the rays' paths as they travel in bent fibers due the geometry change of the original POF as a result of both the ambient temperature and the loading deformation, and consequently induce radiation losses. Furthermore, the stresses within a POF subjected to bending and elongation forces are not distributed uniformly, but vary along the length of the core. The resulting inhomogeneous distribution of the refractive index leads to scattering losses [14]. The higher NA indicates that more modes we have this means that greater radiation and scattering losses this is due to the change in the rays' paths as a result of the loading deformation and inhomogeneous distribution of the refractive index and therefore there are more of them. So the power loss increases in larger NA fibers. Furthermore the power loses in MH-4001 increase rapidly than that in GH-4001. In the same time GH-4001 fiber maintains this improved power loss resistance under high deformation temperature. This is because the GH-4001 fiber has a higher glass transition temperature (Tg) than the MH-4001 fiber. Furthermore it implies that the chain motion in the GH- 4001 is less significant than in the other materials. It means that the polymer chain of the GH-4001 is more inflexible than this of the MH-4001. This is why the power loss increment in the deformed GH-4001 fiber is less than that in the MH-4001 fiber.

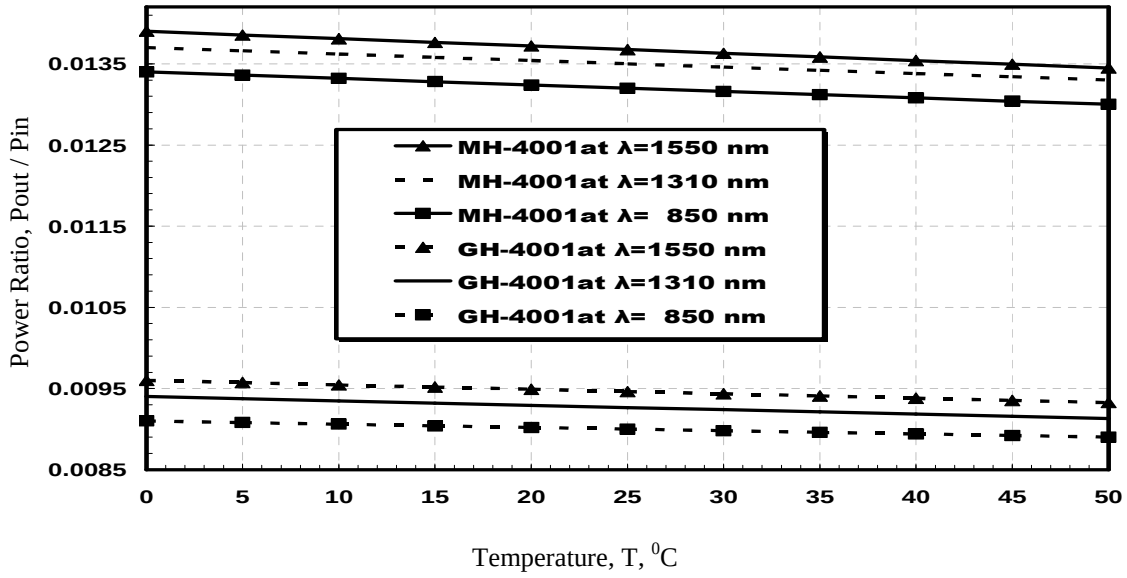

Fig.13. Variations of the power ratio against temperature at different operating wavelengths (λ) with ($\bar{u}_p$ =1 N/mm^2), γ = 0.1 MGy, and NA=0.2.

Figure (13) shows that the power ratio decreases as the value of the operating wavelength (λ) decrease at constant value of average plastic energy density ($\bar{u}_p$ =1 N/mm^2) and radiation dose (γ =0.1 MGy). This result can be attributed to the change in the rays' paths as they travel in bent fibers due the geometry change of the original POF as a result of both the ambient temperature and the loading deformation, and consequently induce radiation losses. Furthermore, the stresses within a POF subjected to bending and elongation forces are not distributed uniformly, but vary along the length of the core. The resulting inhomogeneous distribution of the refractive index leads to scattering losses [14]. the operation at short wavelength means at the same time the operation at high frequency thus the higher frequency, the wider the bandwidth which indicates that more modes we have

which give the ability of sending more complex information this means that greater radiation and scattering losses this is due to the change in the rays' paths as a result of the loading deformation and inhomogeneous distribution of the refractive index and therefore there are more of them. So the power losses increases with increase the bandwidth or decrease the operating wavelength since wider bandwidth indicates that there are more rays that carry information in the fiber**.** However with increasing the temperature which implies that the POF experiences a larger geometrical deformation and thus suffers higher radiation losses. Furthermore the power loses in MH-4001 increase rapidly than that in GH-4001. In the same time GH-4001 fiber maintains this improved power loss resistance under high deformation temperature. This is because the GH-4001 fiber has a higher glass transition temperature (Tg) than the MH-4001 fiber. Furthermore it implies that the chain motion in the GH- 4001 is less significant than in the other materials. It means that the polymer chain of the GH-4001 is more inflexible than this of the MH-4001. This is why the power loss increment in the deformed GH-4001 fiber is less than that in the MH-4001 fiber.

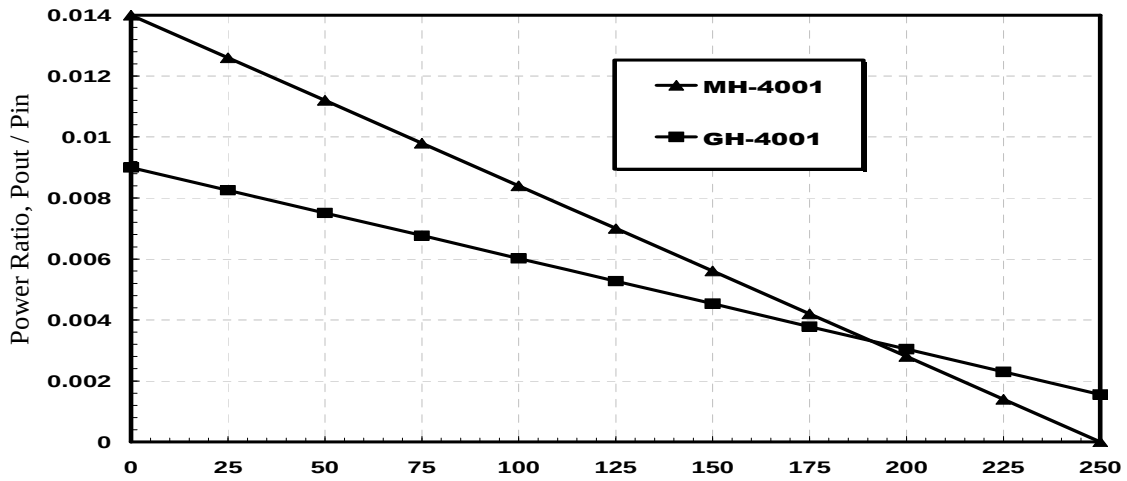

Fig.14. Variations of the power ratio against temperature with ($\bar{u}_p$ =7 N/mm^2), γ=0.1MGy, and λ=1310 nm.

Figure (14) shows that the when the APED increase from 1 to 7 N/mm^2 MH-4001 fiber is still has a higher power ratio than GH-4001 fiber but with increasing the temperature the GH-4001 fiber exhibits a greater resistance to power losses under high APED than MH-4001 fiber. The figure also shows that the two fibers suffers the power ratio decrement with the increasing of the ambient temperature at constant value of average plastic energy density ($\bar{u}_p$ =7 N/mm^2) and radiation dose (γ =0.1 MGy). It is as a result of the change in the rays' paths as they travel in bent fibers due the geometry change of the original POF as a result of both the ambient temperature and the loading deformation, and consequently induces radiation losses. Furthermore, the stresses within a POF subjected to bending and elongation forces are not distributed uniformly, but vary along the length of the core. The resulting inhomogeneous distribution of the refractive index leads to scattering losses [14]. Thus the power losses increases with increase the ambient temperature, Moreover the figure shows also that MH-4001 fiber is a higher power ratio than GH-4001 fiber, at constant low average plastic energy density ($\bar{u}_p$ =7 N/mm^2). Furthermore the power loses in MH-4001 increase rapidly than that in GH-4001. In the same time GH-4001 fiber maintains this improved power loss resistance under high deformation temperature. This is because the GH-4001 fiber has a higher glass transition temperature (Tg) than the MH-4001 fiber. Furthermore it implies that the chain motion in the GH- 4001 is less significant than in the other materials. It means that the polymer chain of the GH-4001 is more inflexible than this of the MH-4001. Moreover with increasing the average plastic energy density which implies that the POF experiences a larger geometrical deformation and thus suffers higher radiation losses the GH-4001 fiber exhibits a greater resistance to power losses under high deformation conditions than MH-4001 fiber. This is due to the diameter shrinkage in the GH-4001 fiber is smaller

than that in the MH-4001 fiber which make the power ratio in the deformed GH-4001 fiber is greater than that in the MH-4001 fiber. The smaller diameter shrinkage and higher glass transition temperature (Tg) interprets why the power loss increment in the deformed GH-4001 fiber is less than that in the MH-4001 fiber at high temperature and APED conditions

.

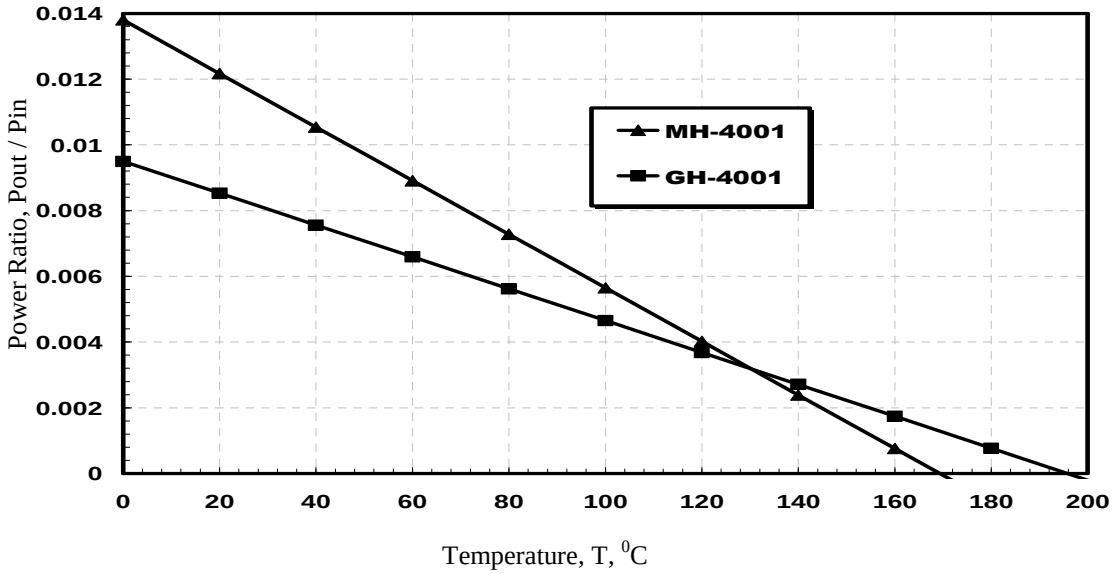

Fig.15. Variations of the power ratio against temperature with ($\bar{u}_p$ =10 N/mm^2), γ=0.1MGy, and λ=1310 nm.

Figure (15) shows that the when the APED increase from 7 to 10 N/mm^2. MH-4001 fiber is still has a higher power ratio than GH-4001 fiber but with increasing the temperature the GH-4001 fiber exhibits a greater resistance to power losses under high APED than MH-4001 fiber. In addition MH-4001 fiber is breakdown faster at temperature lower than in case of figure (14) this is due to increasing APED form 7 to 10 N/mm^2. The figure also shows that the two fibers suffers the power ratio decrement with the increasing of the ambient temperature at constant value of average plastic energy density ($\bar{u}_p$ =10 N/mm^2) and radiation dose (γ =0.1 MGy). It is as a result of the change in the rays' paths as they travel in bent fibers due the geometry change of the original POF as a result of both the ambient temperature and the loading deformation, and consequently induces radiation losses. Furthermore, the stresses within a POF subjected to bending and elongation forces are not distributed uniformly, but vary along the length of the core. The resulting inhomogeneous distribution of the refractive index leads to scattering losses [14]. Thus the power losses increases with increase the ambient temperature, Moreover the figure shows also that MH-4001 fiber is a higher power ratio than GH-4001 fiber, at constant low average plastic energy density ($\bar{u}_p$ =10 N/mm^2). Furthermore the power loses in MH-4001 increase rapidly than that in GH-4001. In the same time GH-4001 fiber maintains this improved power loss resistance under high deformation temperature. This is because the GH-4001 fiber has a higher glass transition temperature (Tg) than the MH-4001 fiber. Furthermore it implies that the chain motion in the GH- 4001 is less significant than in the other materials. It means that the polymer chain of the GH-4001 is more inflexible than this of the MH-4001. Moreover with increasing the average plastic energy density which implies that the POF experiences a larger geometrical deformation and thus suffers higher radiation losses the GH-4001 fiber exhibits a greater resistance to power losses under high deformation conditions than MH-4001 fiber. This is due to the diameter shrinkage in the GH-4001 fiber is smaller than that in the MH-4001 fiber which make the power ratio in the deformed GH-4001 fiber is greater than that in the MH-4001 fiber. The smaller diameter shrinkage and higher glass transition temperature (Tg) interprets why the power loss increment in the deformed GH-4001 fiber is less than that in the MH-4001 fiber at high temperature and APED conditions. In addition by comparing between results of figures 9, 14 and 15 we conclude that fibers have no change in power ratio when higher APED are applied.

IV. CONCLUSION

In this paper a block diagram model treating the radiation and temperature effects on the power losses of bent polymer optical fibers is proposed to provide a mean to control the optical properties of fibers in radiation environments. The radiation dose and the temperature dependence of power losses for the optical fibers were studied by using VisSim environment for radiation dose ranging from 0.1-3.0 MGy and temperature ranging from 25^0C-80^0C. The effect of clad refractive index, numerical aperture, operating wavelength under radiation and temperature condition on the power ratio that shows a high contribution in the performance of the optical fiber links is demonstrated. Furthermore the results have revealed that the GH-4001 POF exhibits a greater resistance to power losses under high radiation, temperature and loading deformation conditions than MH-4001.

REFERENCES

[1] M. S. Kovacevic´, S. Savovic´, A. Djordjevich , J. Bajic´ , D. Stupar, M. Kovacevic´, and S. Simic´, "Measurements of growth and decay of radiation induced attenuation during the irradiation and recovery of plastic optical fibres", Optics and Laser Technology, Vol. 47, pp. 148–151, 2013.

[2] R. Guobin, W. Zhi, L. Shuqin, and J. Shuisheng, "Analysis of dispersion properties of high-index-core Bragg fiber", Optical Fiber Technology, Vol. 11, pp. 81–91, 2005.

[3] F. El-Diasty, H. A. El-Hennawi, and M. A. Soliman, "Chromatic and opto -mechanical dispersion of some characteristic parameters of optical fiber undergoing macrobending", Optics Communications, Vol. 267, pp. 394–401, 2006.

[4] J. Crisp, "Introduction to fiber optics", Newnes, 2001.

[5] M. A. Losada, I. Garcés, J. Mateo, I. Salinas, J. Lou, and J. Zubía, "Mode coupling contribution to radiation losses in curvatures for high and low numerical aperture plastic optical fibers", Journal of Lightwave Technology, Vol. 20, pp. 1160-1164, 2002.

[6] S. E. Golowich, W. White, W. A. Reed, and E. Knudsen, "Quantitative estimates of mode coupling and differential modal attenuation in perfluorinated graded-index plastic optical fiber", Journal of Lightwave Technology, Vol. 21, pp. 111-121, 2003.

[7] J. Zubia and J. Arrue, "Plastic optical fibers: an introduction to their technological processes and applications", Optical Fiber Technology, Vol. 7, pp. 101-140, 2001.

[8] S. O'Keeffe, and E. Lewis, "Polymer optical fiber for in situ monitoring of gamma radiation processes", International Journal on Smart Sensing and Intelligent Systems, Vol. 2, pp. 490-502, 2009.

[9] l. A. S. de Oliveira and M. Bonfim, "Plastic optical fibers in telecommunications: analysis, comparison and applications", IEEE Transactions on Nuclear Science, Vol. 5, pp. 651-655, 2003.

[10] Y. C. Chen, "Power losses in deformed polymer optical fiber under high temperature", Journal of Lightwave Technology, Vol. 24, pp. 4983-4990, 2006.

[11] K. Makino, T. Ishigure, and Y. Koike, "Waveguide parameter design of graded-index plastic optical fibers for bending-loss reduction", Journal of Lightwave Technology, Vol. 24, pp. 2108-2114, 2006.

[12] J. P. Powers, "An introduction to fiber optic systems", Mc graw-hill, 1986.

[13] D. Jones, "Introduction to fiber optics", Naval Education and Training Professional Development and Technology Center, 1998.

[14] L. W. Chen, W. H. Lu, Y. C. Chen, "An investigation into power attenuations in deformed polymer optical fibers under high temperature conditions", Optics Communications, Vol. 282, pp. 1135–1140, 2009.

[15] S. Share and J. Wasilik," Radiation effects in doped-silica optical waveguides", IEEE Transactions on Nuclear Science, Vol. 26, pp. 4802-4807, 1979.

[16] M. C. Paul, R. Sen, S. K. Bhadra, M. Pal, P. P. Giri, K. Disgusts, T. K. Bandyopadhyay, D. Bohra and P. K. Bhatnagar, "Gamma ray radiation induced absorption in Ti doped single mode optical fibres at low dose levels", Optical Materials, Vol. 29, pp. 738–745, 2007.

[17] F. Liu, Y. An, P. Wang, B. Shao and S. Chen, "Effects of radiation on optical fibers", Journal of Recent Progress in Optical Fiber Research, Vol. 6 ,pp. 431-451, 2012.

[18] D. Sporea, A. Sporea, S. O'Keeffe, D. M. Carthy and E. Lewis "Optical fibers and optical fiber sensors used in radiation monitoring", Journal of Optical Fiber Technology, Vol. 51, pp. 607-653, 2012.

[19] E. F. Alfaro, D. B. Dias, and L. G. A. Silva, "The study of ionizing radiation effects on polypropylene and rice husk ash composite", Journal of Radiation Physics and Chemistry, Vol. 6, pp. 25–27, 2012.

[20] P. Y. Inamura, F. H. Kraide, W. S. Drumond, N. B. D. Lima, E. A. B. Moura, and N. D. Mastro, "Ionizing radiation influence on the morphological and thermal characteristics of a biocomposite prepared with gelatin and Brazil nut wastes as fiber source", Journal of Radiation Physics and Chemistry, Vol. 6, pp. 43–46, 2012.

[21] W. P. Ferro, L. D. Gondim de Andrade, and L. G. A. Silva, "Ionizing radiation effect studies on polyamide 6.6 properties", Radiation Physics and Chemistry, Vol. 71, pp. 267–269, 2004.

[22] M. M. Nasef, and E. A. Hegazy, "Preparation and applications of ion exchange membranes by radiation-induced graft copolymerization of polar monomers onto non-polar films", Progress in Polymer Science, Vol. 29, pp. 499–561, 2004.

[23] J. A. Wall, and J. F. Bryant, "Radiation effects on fiber optics", Journal of Physical Sciences Research Papers, Vol. 75, pp.1-54, 1975.

[24] [24] A. J. Baba, S. Share and J. H. Wasilik' "Effects of simulated nuclear thermal pulses on fiber optic cables", IEEE Transactions on Nuclear Science, Vol. 26, pp. 4792-4795, 1979.

[25] K. A. Murray, J. E. Kennedy, B. M. Evoy, O. Vrain, Damien Ryan, and Clement L. Higginbotham, "Effects of gamma ray and electron beam irradiation on the mechanical, thermal, structural and physicochemical properties of poly (ether-block-amide) thermoplastic elastomers", Journal of the Mechanical Behavior of Biomedical Materials, Vol. 12, pp. 255-306, 2012.

[26] R. ElAbdi, A. Rujinski, M. Poulain, and I. Severin, "Silica optical fiber behavior under x-rays and microwaves", Optics and Lasers in Engineering, Vol. 47, pp. 519–526, 2009.

[27] X. Feng, F. Poletti, A. Camerlingo, F. Parmigiani, P. Petropoulos, P. Horak, G. M. Ponzo, M. Petrovich, J. Shi, W. H. Loh, and D. J. Richardson, "Dispersion controlled highly nonlinear fibers for all optical processing at telecoms wavelengths", Optical Fiber Technology, Vol. 16, pp. 378–391, 2010.

[28] A. N. Z. Rashed, "Harmful effects of gamma irradiation on optical Fiber communication system links under thermal environment effects", International Journal on Electronics and Communication Technology, Vol. 3, pp. 71–75, 2012.

[29] P. S. Andre, A. N. Pinto, and J. L. Pinto, "Effect of temperature on the single mode fibers chromatic dispersion", IEEE, Vol. 5, pp. 231–234, 2003.